Optimizing the FOCI algorithm with a weighted least-squares approach

Saleh Al-Saleh and Gary Margrave, University of Calgary*

Summary

Recursive wavefield extrapolation methods can effectively handle lateral velocity variations, but require short stable operators to be computationally efficient. The forward operator and conjugate inverse (FOCI) algorithm can be used to design sufficiently stable wavefield extrapolators. However, the FOCI algorithm generally requires long operators to generate good images. In this paper we present an enhanced FOCI algorithm that uses weighted least-squares. With the optimized algorithm it is possible to design operators as short as 9 points that can remain practically stable in a recursive scheme. Zero-offset migration impulse responses and images from prestack depth migrations of the Marmousi dataset are used to compare the effects of these enhancements to results from the original algorithm.

Introduction

Wavefield extrapolation in 2D can be done in the space-frequency domain as a non-stationary convolution (Margrave et al., 2006)

$$\psi(x,z+\Delta z,\omega)=\int_{-\infty}^{\infty}\psi(x',z,\omega)W(x-x',k(x),\Delta z)\,dx'. \quad (1)$$

The non-stationary operator is given by

$$W(x-x',k(x),\Delta z)=$$

$$\frac{1}{2\pi}\int_{-\infty}^{\infty}\hat{W}(k_x,k(x),\Delta z)e^{-ik_x(x-x')}dk_x, \quad (2)$$

where

$$\hat{W}(k_x,k(x),\Delta z)=\exp\left(i\Delta z\sqrt{k(x)^2-k_x^2}\right) \quad (3)$$

and

$$k(x)=\frac{\omega}{v(x)}. \quad (4)$$

ψ is the pressure wavefield after taking its Fourier transformation over the temporal coordinate, z is depth, Δz is the depth increment, ω is the temporal frequency, k_x is the transverse wavenumber, x' denotes the transverse coordinate at input, x denotes the transverse coordinate at output, and $v(x)$ is the space-variant velocity field. When the velocity is constant, equation 1 becomes the space-frequency equivalent of Gazdag's (1978) phase-shift migration. The non-stationary convolution operator, W, handles lateral velocity variations by using a different operator for each output point. Developing a fast and efficient wavefield extrapolation method from equation 1 requires finding a compactly supported approximation, $\tilde{W}$, to the ideal response, W, which is infinitely long. Using simple window functions such as a boxcar or a Hanning window to truncate the infinitely long extrapolator result in operators that either amplify or decay the wavefield when they are used recursively (Thorbecke et al., 2004). There are different methods for designing wavefield extrapolators, e.g. Holberg (1988), Hale (1991), Soubaras (1996), Thorbecke et al. (2004), and Al-Saleh et al. (2006). Most extrapolation methods design operators that have practical stabilities. That is, the operators are not perfectly stable, but have controlled instabilities.

We present an enhanced version of the FOCI algorithm (Margrave et al., 2006) by using a weighted least-squares approach. The theory of these enhancements will be followed by a series of examples and comparisons between the old and new designs, beginning with operator amplitude and phase spectra, impulse responses, and finally pre-stack depth migration results. The full migrations are all done on 2-D acoustic Marmousi model.

Theory

In the FOCI algorithm (Margrave et al., 2006), two operators are used: (1) a forward operator obtained from windowing the ideal operator for a half step, and (2) an inverse operator that is designed as the band-limited inverse of the forward operator. The least-squares FOCI operator is formed by convolving the first operator with the conjugate of the second. This FOCI operator can also be windowed to generate a shorter post-design operator. To optimize the algorithm, the suboptimal windowing is replaced with a weighted least-squares approach.

The amplitude and phase spectra of the desired transform, $\hat{W}$, have discontinuities at boundaries separating the wavelike and evanescent regions. Most extrapolation methods modify the desired transform in such a way that it does not have these sharp changes. Al-Saleh et al. (2006) modify the desired transform in the weighted least-squares with a transition band (WLSTB) approach. The band of wavenumbers for the transition region that contains the discontinuities is thereby simply removed from the error definition (Parks and Burrus, 1987; Selesnick et. al., 1996). The width of this region depends on the maximum angle of propagation, α, which is a user defined parameter. The WSLTB approach can be used in FOCI to obtain the

The enhanced FOCI algorithm

forward and the post-design operators in an optimal way. Thus instead of using a Hanning window to obtain the forward operator, the WLSTB is used:

$$\tilde{\underline{W}} = \left[\underline{F}^H \underline{\Upsilon} \underline{F} \right]^{-1} \underline{F}^H \underline{\Upsilon} \hat{\underline{W}} , \tag{5}$$

where

$$\Upsilon(k_x, \omega) = \begin{cases} 1 & |k_x| \le k_\alpha \\ 0 & k_\alpha < |k_x| < |2k - k_\alpha| \\ \varepsilon(\omega) & |2k - k_\alpha| < |k_x| < \dfrac{\pi}{\Delta x} \end{cases} , \tag{6}$$

$0 < \varepsilon(\omega) \ll 1$, the subscript "_" denotes a matrix, "^" symbolizes the Fourier transform over the spatial coordinates, $k_\alpha = k(x)\sin\alpha$, and M is the number of samples of the Fourier transform. N is the number of filter coefficients, the superscript "H" denotes the complex-conjugate transpose, $\underline{F}$ is an N by M subset of the Fourier transformation matrix, and $M \ge N$ (the equations are generally more specified than unknowns). Note that the weight function depends on the frequency; that is, for more stable designs, operators that correspond to different frequencies may require different ε values. The inverse operator can be then obtained as a band limited inverse to the forward operator

$$\tilde{W}_I \bullet \tilde{W}(\Delta z/2) = F^{-1}\left[\left| \hat{W}(\Delta z/2) \right| \right] . \tag{7}$$

Once the inverse operator is solved for using least-squares, the enhanced FOCI operator can be assembled using

$$W_F(\Delta z) = \tilde{W}_I^* \bullet \tilde{W}(\Delta z/2) , \tag{8}$$

where "*" indicates the complex conjugate. An optimally designed post-design operator is then calculated as

$$W_P = \left[\underline{F}^H \underline{\Upsilon} \underline{F} \right]^{-1} \underline{F}^H \underline{\Upsilon} \hat{\underline{W}}_F , \tag{9}$$

where the number of coefficients of W_P may not exceed the number of coefficients in W_F. Note that now the desired transform, $\hat{W}_F$, is the spatial Fourier transform of the FOCI operator, which means that W_P is the smooth version W_F in a least-squares sense. Thereby, using the WLSTB in FOCI makes the algorithm more optimal and efficient. Further, it is now possible to design very short operators which have both practical stability and strong evanescent filtering.

Discussion

Figure 1a shows the amplitude spectra of the Fourier transforms of the post-design operators before and after the enhancement. The optimized operator has a wider spectrum and a better stability than the old design and can better handle high angles of propagation. Also, the phase of the optimized operator better approximates the phase of the exact transform (Figure 1b).

Figure 2 shows a comparison of the impulse responses of post-stack implementations of the phase-shift algorithm (Figure 2a), the original FOCI algorithm (Figure 2b), and the optimized FOCI algorithm (Figure 2c). The input was a set of six impulses on the center trace, the velocity was 4000 m/s, and the trace spacing and depth step were both 10 m. The enhanced algorithm improves the response compared to the old design. The results were obtained with 15 points post-design operators. Such a short operator, when obtained with the old algorithm, cannot handle high angles of propagation, as expected based on its amplitude spectrum (Figure 1a).

The Marmousi dataset has strong lateral velocity variations and steeply dipping events which makes it an ideal dataset to test the accuracy of wavefield extrapolators (Bourgeois et al., 1991). Prestack depth migrations of this dataset are done using the FOCI algorithm before and after the enhancements with 15 point post-design operators. The dataset consists of 240 individual shot records of 96 traces, each in a marine streamer configuration. The source and receiver intervals are 25 m, and the highest coherent frequencies in the data are about 50 Hz. Prior to migration, each shot was interpolated to a receiver spacing of 8.3333 m. Figure 3a shows an approximation to the Marmousi reflectivity. The migration results of the FOCI and enhanced FOCI algorithms are shown in Figures 3b and 3c. Figure 4 shows close-ups of the central parts of Figure 3a, Figure 3b, and Figure 3c. These figures show that the image obtained with the enhanced algorithm is in better agreement with the reflectivity. Further, it shows more details of the Marmousi dataset than the image obtained with the original algorithm where the target reservoir and the dipping events were better resolved. Moreover, with the enhanced algorithm, it is possible to obtain a very good image (Figure 5) with a very short operator, such as, 9 points. These figures show that the optimized FOCI algorithm is now more efficient and accurate.

Conclusions

The forward operator and conjugate inverse (FOCI) algorithm uses Wiener filtering to design wavefield extrapolators that remain practically stable in a recursive scheme. The old algorithm used suboptimal windowing and thus required long operators to generate good images. Using a weighted least-squares approach to replace the use of a Hanning window in the old design makes the algorithm more optimal. With the enhanced algorithm, it is possible to design short operators that remain practically stable in a recursive scheme. Further, this enhancement eliminates the

need for dual tables for evanescent filtering, since the operator can attenuate the evanescent energy very effectively.

References

Al-Saleh, S. M., G. F. Margrave, and J. C. Bancroft, 2006, Designing wavefield extrapolators using a weighted least-squares, CSEG Annual convention, Calgary, AB., Expanded Abstracts, 4 pages.

Bourgeois, A., M. Bourget, P. Lailly, M. Poulet, P. Ricarte, and R. Versteeg, 1991, Marmousi, model and data: in Versteeg, R. and Grau, G. (editors), 1991, The Marmousi experience, Proceedings of the 1990 EAGE workshop on practical aspects of seismic data inversion, EAGE, 5-16.

Gazdag, J., 1978, Wave equation migration with the phase-shift method: Geophysics, **43**, 1342-1351.

Hale, D., 1991, Stable explicit depth extrapolation of seismic wavefield: Geophysics, **56**, 1770-1777.

Holberg, O., 1988, Towards optimum one-way wave propagation: Geophys. Prosp., **36**, 99-114.

Margrave, G. F., H. D. Geiger, S. M. Al-Saleh, and M. P. Lamoureux, 2006, Improving explicit depth migration with a stabilizing Wiener filter and spatial resampling: Geophysics, accepted.

Parks, T. W., and C. S. Burrus, 1987, Digital Filter Design, John Wiley & Sons, 54-83.

Selesnick, I. W., M. Lang, and C. S. Burrus, 1996, Constrained Least Squares Design of FIR Filters with Specified Transition Band:, IEEE, **44**, 1879-1892.

Soubaras, R., 1996, Explicit 3-D migration using equiripple polynomial expansion and Laplacian synthesis: Geophysics, **61**, 1386-1393.

Thorbecke, J., K. Wapenaar, and G. Swinnen, 2004, Design of one-way wavefield extrapolation operators, using smooth functions in WLSQ optimization: Geophysics, **69**, 1037-1045.

Acknowledgements

We wish to thank the sponsors of the CREWES project and the POTSI project. We also specifically thank NSERC, MITACS, and PIMS for providing funding and other support. We would like also to thank Saudi Aramco Oil Company. We also thank Chuck Ursenbach and Hugh Geiger for their comments and suggestions.

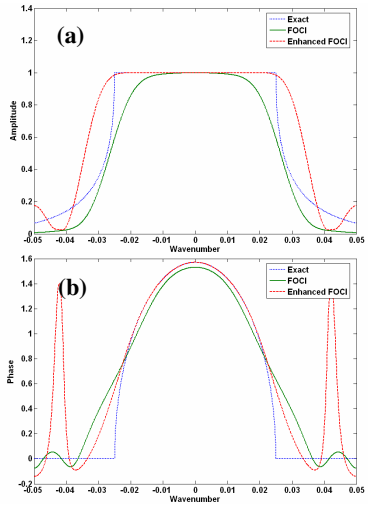

Figure 1: Shows (a) amplitude and (b) phase spectra of the forward operator before and after the enhancement.

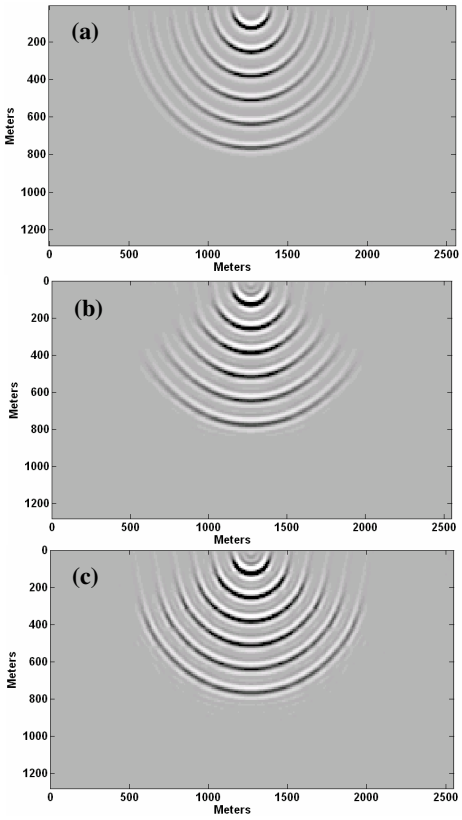

Figure 2: Impulse responses of (a) phase-shift, (b) original FOCI, and (c) enhanced FOCI. The results were obtained using 15 points operators.

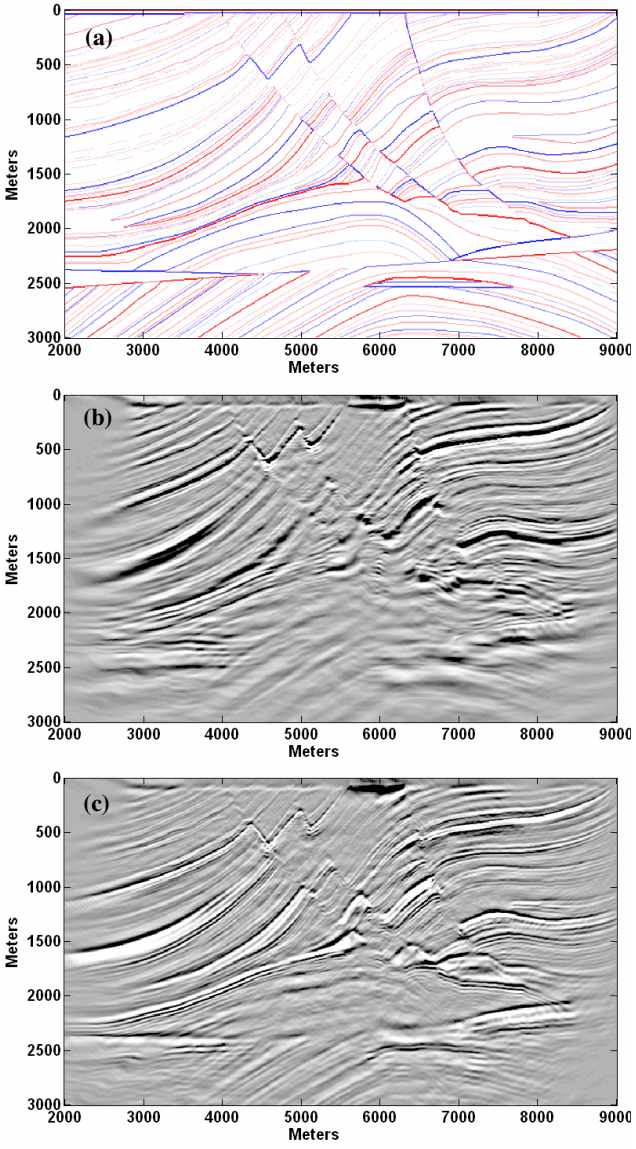

Figure 3: Prestack depth migration results of Marmousi dataset where (a) shows the reflectivity, (b) shows the result of the original FOCI algorithm, and (c) shows the result of the enhanced FOCI algorithm.

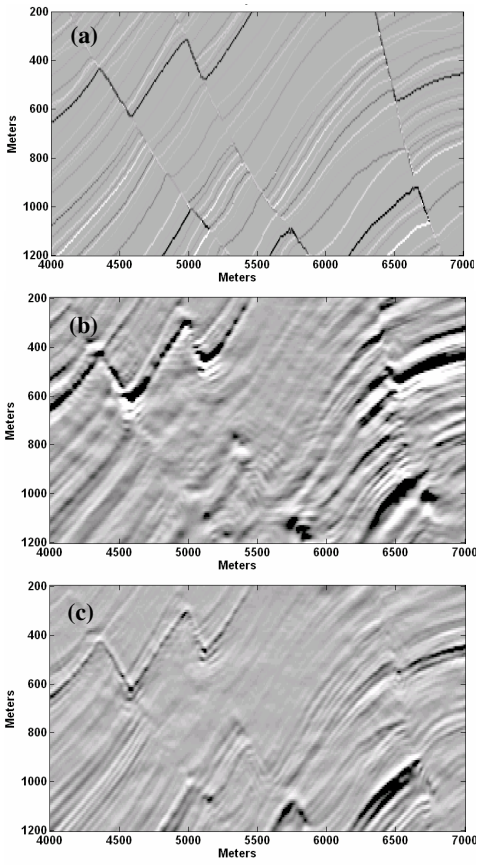

Figure 4: Close-up views of the shallow central sections of Figures 3a, 3b, and 3c.

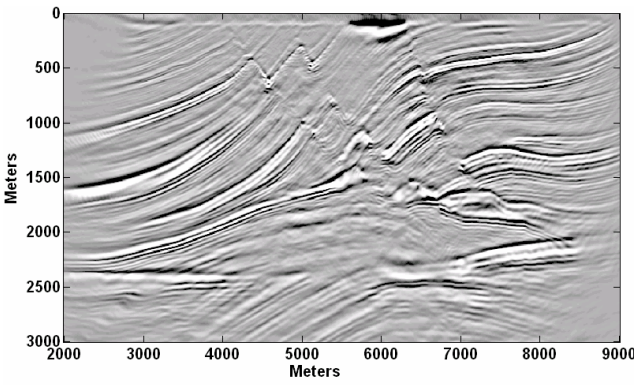

Figure 5: Prestack migration result obtained with the enhanced FOCI algorithm using a 9 points operator.